IEEE Access
Multidisciplinary | Rapid Review | Open Access Journal

Received July 4, 2019, accepted July 18, 2019, date of publication July 24, 2019, date of current version August 9, 2019.

Digital Object Identifier 10.1109/ACCESS.2019.2930673

Design of a Novel Compact Slotted Cavity With Shaped Beam for High Power Microwave Feed Antenna Using Asymmetric High Order Mode

XIAO MA, (Student Member, IEEE), FENG YANG, (Member, IEEE), PENG YANG, (Member, IEEE), RUI WANG, YI YAN, (Student Member, IEEE), AND KEXIU CHEN

School of Electronic Science and Engineering (National Exemplary School of Microelectronics), University of Electronic Science and Technology of China (UESTC), Chengdu 611731, China

Corresponding author: Feng Yang (yangf@uestc.edu.cn)

This work was supported in part by the National Natural Science Foundation of China under Grant 61871101 and Grant 61721001, in part by the National Key Research and Development Program of China under Grant 2016YFC0303501, and in part by the Joint Fund of Equipment Pre-Research of Aerospace Science and Technology under Grant 6141B061008.

ABSTRACT In order to achieve a shaped beam on a compact aperture and reduce the cost and the volume, a conformal slotted cavity as a feed antenna for high-power microwave using the asymmetric high-order mode is investigated. The proposed antenna working in a high-order mode has merits on reducing the complexity of a power network and the volume of a mode converter. The alternate arrangement of the slot array is taken into account, and the asymmetric high-order mode TE_{430} is selected to improve the symmetry of far-field pattern at the *E*-plane. A novel design of wide slot with the horn-cavity etched on the top surface of the upper cavity achieves the uniform aperture field and mitigates the maximum electric field enhancement, and calculated results verify that the proposed antenna is capable of high-power handling capability (above 1.29 GW in vacuum). The conformal slot array is introduced to obtain a shaped beam, which helps to illuminate reflect array with shaped aperture efficiently. The simulation and measured results show that the feed antenna achieves a low-profile structure of $2.4\lambda_0 \times 2.8\lambda_0 \times 0.8\lambda_0$, the 10-dB gain beamwidth of *E*-plane is 56.6° at the operating frequency of 9.1 GHz, the maximum difference of the gain, and the 10-dB beamwidth angle between the two sides of main beam is no more than 1 dB and 1°, respectively.

INDEX TERMS Asymmetric high order mode, shaped beam, compact feed antenna, conformal array, high power microwave, horn-cavity, power handling capability, slotted cavity.

I. INTRODUCTION

High power microwave (HPM) technology is a new subject with the development of the pulse power technology in 1970s that has important research value in high energy physics and defense military application. The HPM antenna technology has attracted more attention from researchers as a bottleneck for the rapid development of HPM source technology.

The common HPM antennas are shown in Fig. 1. Obviously, the volume and cost of HPM antennas are higher than the traditional microwave antennas. The defect of no electronic scan gradually becomes the main problem faced by the HPM antenna technology [1]–[13]. In a few decades ago, Vlasov antenna [1] as a feed antenna in HPM features a simple structure, easy manufacture, and high power capacity. However, the application of the antenna is in general limited by its off-axis beam. At present, horn antennas with high power capacity are often used as feed antennas in HPM [8]–[13], which can achieve effective radiation in the axial direction by cascading with a mode converter or an overmoded section. With the rapid development of the HPM technology, especially the technological breakthroughs achieved by the HPM source technology in recent years, many new requirements have been put forward for the HPM antenna technology. Miniaturization, low power capacity and high cost are new problems that need to be solved in HPM antenna technology.

Compared with traditional microwave antennas, the difference in design of HPM antennas is mainly reflected in the output mode of the HPM source, the transmission mode of the feedline, and the power capacity.

The associate editor coordinating the review of this manuscript and approving it for publication was Luyu Zhao.

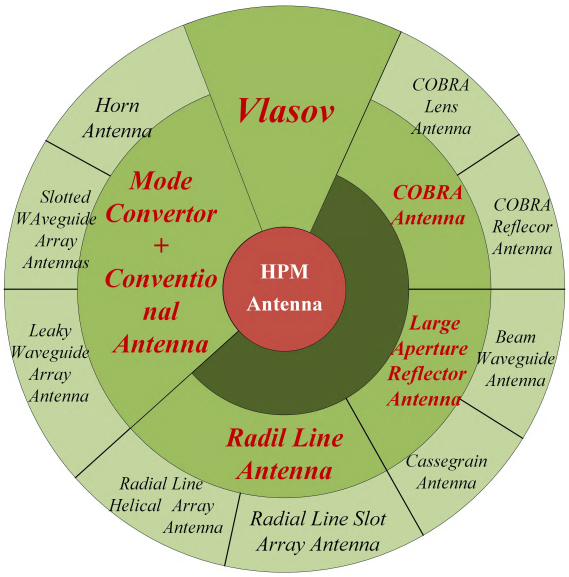

FIGURE 1. The family tree of the traditional HPM antennas.

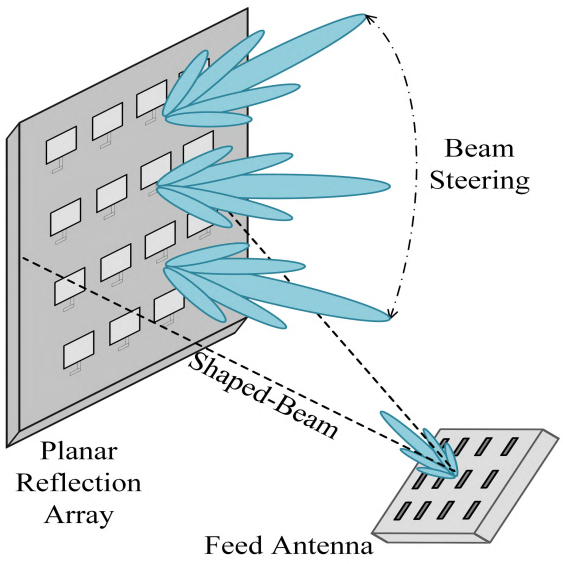

FIGURE 2. Application on the shaped beam antenna in HPM.

HPM sources (such as magnetically insulated wire oscillator, MILO [19]) couple the spin electron beam energy into radio frequency energy by means of the slow wave structure, so the output electromagnetic (EM) wave also works in rotationally symmetric mode, such as TM_{0n} and TEM mode. A cascaded mode converter is required to convert TM_{0n} or TEM mode into TE_{11} mode that can achieve axial radiation. However, the radial [20], [22] or lateral [21] dimensions of mode converters are typically one or several free space wavelengths, which increases the volume of the antenna. In addition, the EMP bomb illuminates on the specified area using a horn antenna, and limitations on load and space of the missile pose a new challenge to the HPM antenna technology.

The dielectric material and the discontinuous abrupt structure can cause the EM field to be compressed, which directly represents as the enhancement of electric field and is the main cause of dielectric (air) breakdown. When the dielectric (air) is ionized, plasma begins to accumulate rapidly. When the HPM passes through the plasma, it makes the HPM pulse width short, transmission energy drops, and then the HPM is refracted, reflected, absorbed, even can damage the HPM source [14]. Therefore, low power microwave devices (such as ferrite phase shifters) [16]–[18] are difficult to applied in HPM. In addition, the verification process of power capacity is an extremely complex interdisciplinary problem. At present, the power capacity is estimated by calculating formulas based on simulation results. This is not the main research content of this paper, and will not be discussed. In the design of HPM antennas, it is not only necessary to follow the design method of the traditional microwave antenna, but also to solve the problem of power capacity by effective methods. Therefore, as indicators increase, the design difficulty will also increase.

Both slot array antenna and slotted cavity antenna fed by narrow gap or coaxial line have the advantage of a low profile. However, gaps and coaxial lines are difficult to transmit the HPM energy. In order to transmit higher energy, HPM sources typically use the overmoded circular waveguide [22] or coaxial waveguide (CWG) [23] as the transmission waveguide. The nonstandard overmoded transmission waveguide operates in high order modes, and improves the power capacity at expense of the lateral cross-sectional dimensions or overmode ratio (ratio of the outer conductor diameter to the inner conductor diameter). Compared with the conventional coaxial line, the cross-section dimension of the overmoded CWG is typically larger than half of the operating wavelength of the cavity. Therefore, it is difficult for the overmoded CWG to excite high order modes in the cavity by means of an electric probe. When it is directly cascaded with the slotted cavity antenna, high order interference modes (IMs) excited by the discontinuity cause a great disturbance to the operating mode.

In order to obtain the best aperture efficiency, the HPM reflectarray antenna with a shaped aperture needs to be illuminated by the feed antenna that has a shaped beam, as seen in Fig. 2. At present, no horn antenna with shaped beam as a feed antenna in HPM has been reported in papers. The horn antenna reported in [24] obtains an isoflux beam by parasitic elements. However, the parasitic element belongs to a discontinuous abrupt structure, which tends to the excessive concentration of the electric field, and decrease the power capacity. On the other hand, since the slot array achieves effective gain in the far field by means of an alternate arrangement, it is difficult to obtain a symmetric far field pattern of E-plane on a compact aperture [25], which reduces the radiation efficiency of the reflectarray antenna as well. The asymmetric high order mode (AHOM) has been proposed to improve the symmetry of far field pattern at E-plane in [26]. The even high order mode TE_{506} has an even number of standing wave peaks along E-plane to overcome the asymmetry.

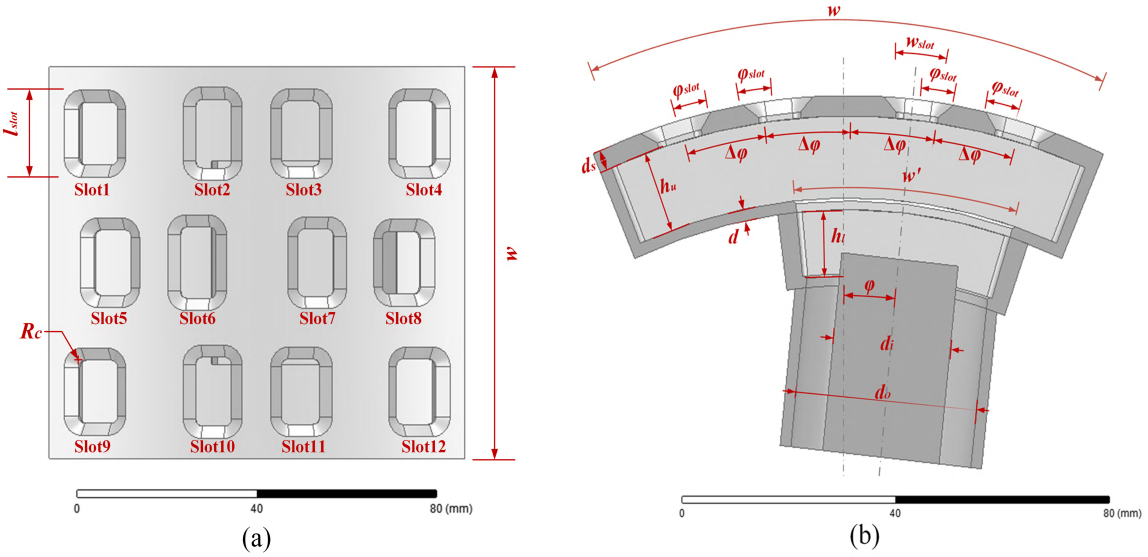

FIGURE 3. Top and cross-section views of the proposed slotted cavity feed antenna: (a) top view; (b) cross-section view.

As a radiation element, the slot is the main reason for limiting the power capacity of the slotted cavity antenna. A narrow slot can cause the concentration of the electric field, but a wide slot can increase the mutual coupling within the array and deteriorate the radiation performance of the antenna. Although chamfer, fillet and other methods [35], [36] are essential, the calculation of the minimum width of slot that avoid air breakdown helps to accurately estimate the power capacity of the antenna.

This paper innovatively designs a compact feed antenna in HPM. Compared with the conventional HPM horn antenna, the feed antenna proposed in this paper achieves the shaped beam on a compact aperture using the conformal technology [37], which has advantages of volume reduction and power capacity improvement. As seen in Table 2, axial size and aperture area is reduced by at least 76% and 50%, respectively. The proposed antenna improves the asymmetry of the E-plane pattern of the compact slot array antenna using the AHOM (TE_{430}). The maximum gain difference within the 10-dB beamwidth is less than 1 dB. The EM field operating in high order mode has a characteristic of power distribution, eliminating the need for additional power dividers, phase shifters and mode converters. It can be directly cascaded with the HPM source through the overmoded CWG to achieve a low profile. This study innovatively designs a conformal slotted cavity that can simultaneously operates in two high order modes to mitigate the effects of IMs excited by the overmoded CWG on the operating mode. The design of the wide slot integrated with horn cavity decreases the probability of air breakdown, and improves the power capacity. The simulation results show that the power capacity is above 1.29 GW.

The organization of this paper is as follows: The antenna configuration and the detail dimension are listed in Section II. The radiation power estimation of the slot and the theory of cavity mode are described in Section III. Under the guideline theory of conformal array, the novel slotted cavity antenna with shaped beam for feed is described, and the horn-cavity slot is introduced and the power handling capability is discussed in Section IV. The simulation and measured results are shown in Section V. Finally, a comprehensive summary is given in Section VI.

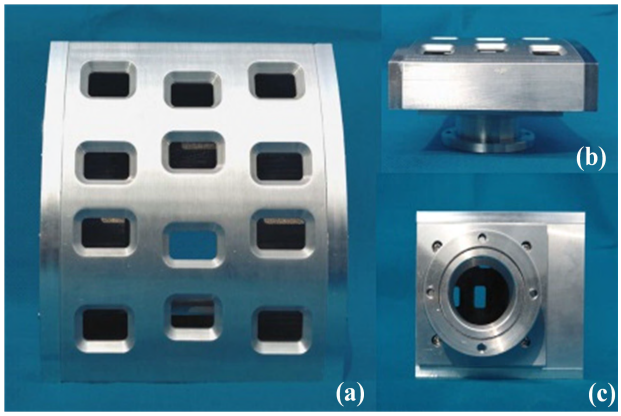

FIGURE 4. Photographs of the manufactured HPM feed antenna: (a) top view; (b) side view; (c) bottom view.

II. ANTENNA CONFIGURATION

The structure of the proposed antenna is shown in Fig. 3, which has a compact size of $2.4\lambda_0 \times 2.8\lambda_0 \times 0.8\lambda_0$, and consists of a conformal slotted cavity and an overmoded coaxial waveguide that are direct connected. The slot array with the horn-cavity is etched on the top surface of the cavity. Chamfer and fillet have been done for each slot. The whole structure is fabricated with metal, and no microwave dielectric material is used. Then, the top, the side and the bottom views of the manufactured antenna are shown in Fig. 4. The detailed dimensions are listed in Table 1.

TABLE 1. Dimensions of the proposed antenna.

Symbol	Quality	Value
w	edge length of the upper cavity	79.8 mm
l_{slot}	length of the 12 slots	13mm,14.5mm,14mm,13.5mm, 13.5mm,14.75mm,13mm,13mm, 13mm,14mm,14mm,13.5mm
w_{slot}	width of the 12 slots	8mm,7.25mm,7.75mm,8mm, 7.5mm,7.25mm,7mm,7.5mm, 78mm,7.25mm,7.5mm,8mm
w'	edge length of the lower cavity	42 mm
d	thickness of the cavity	0.5 mm
d_s	thickness of the horn-cavity	3.5 mm
h_u	height of the upper cavity	14 mm
h_l	height of the lower cavity	13 mm
d_i	diameter of the inner conductor	11.7 mm
d_o	diameter of the outer conductor	17 mm
R_c	fillet dimension of all the horn-cavity and the slot	17 mm
φ	curvature angle	45°
$\Delta\varphi$	segmental angle (spacing angle)	6.38°
φ_{offset}	offset distance of each slot	0.83°

III. THEORY OF CAVITY MODE

A. POWER CAPACITY OF RADIATION UNITS

In [27], the maximum field enhancement factor (MFEF) is introduced to straightly represent the enhancement degrees of the electric field, and is determined by the ratio of the maximum electric field ($E_{\max}$) to the electric field of the incident electromagnetic wave (E_0). The detailed expression is as follows:

$$\mathbf{MFEF} = \frac{E_{\max}}{E_0}. \tag{1}$$

It makes quantitative estimation on power handling capability. As referred above, dielectric breakdown is a complex process including electric breakdown, thermal breakdown, and partial discharge, which occurs over time [15]. Although the solid dielectric has the highest dielectric strength (DS), the solid dielectric breakdown is an irreversible process. Once it happens, the solid dielectric will be damaged and cannot be recovered. Therefore, gas dielectric with self-healing ability (especially vacuum or SF_6 gas) will be the optimal choice of the dielectric for HPM.

In general, the DS can be calculated by the operating frequency and $E_{\max}$ using *Kilpatrick* rule [28], and is shown as

$$f = 1.64\mathrm{DS}^2 e^{-\frac{8.5}{E_{\max}}}. \tag{2}$$

In the X-band, the DS in vacuum is about 74-89.7 MV/m. The expression for calculating the maximum power capacity of rectangular waveguide (RWG) working in fundamental transmission mode, is defined by

$$\mathrm{P}_{max} = \frac{ab}{4\eta}\sqrt{1-\left(\frac{\lambda}{\lambda_c}\right)^2}E_{max}^2. \tag{3}$$

where, the free space wave impedance $\eta = \sqrt{\frac{\mu}{\varepsilon}}$, λ and λ_c are space wavelength and cutoff wavelength, respectively.

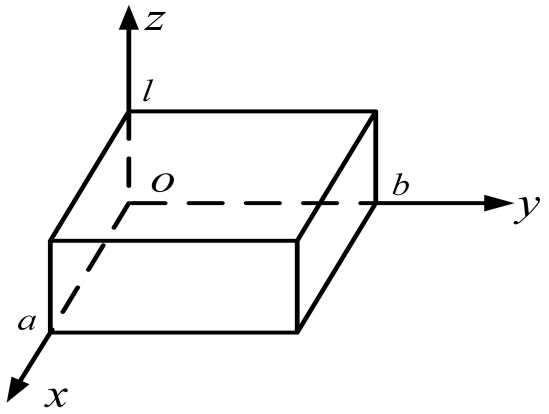

FIGURE 5. Sketch of the square cavity.

a and b are side length of RWG. Suppose the device is working in vacuum without dielectric breakdown, then the power capacity can be determined by $E_{\max}$ in air, as shown below:

$$P_{est} = \frac{a'_{est}b'_{est}l'_{est}}{a'_{sim}b'_{sim}l'_{sim}} \cdot \frac{\sqrt{1-\left(\frac{\lambda_{est}}{\lambda_{c,est}}\right)^2}}{\sqrt{1-\left(\frac{\lambda_{sim}}{\lambda_{c,sim}}\right)^2}} \cdot \frac{E_{max,est}^2}{E_{max,sim}^2} \cdot P_{sim}, \tag{4}$$

where, the subscript 'est' and 'sim' represent the estimated and simulation values, respectively. P is the sign of power capacity. a', b' and l' are side length of the cavity, as seen in Fig. 5. Extended to the proposed antenna, the first term on the right-hand side can be replaced by volume. For this example, the relationship is as follows: $a'_{est} = a'_{sim}, b'_{est} = b'_{sim}, l'_{est} = l'_{sim}, \lambda_{est} = \lambda_{sim}, \lambda_{c,est} = \lambda_{c,sim}$. Then, the estimation on power capacity of the proposed antenna in vacuum can be calculated directly by the simulated maximum electric field in air ($E_{max,sim}$), the simulated power of the incident EM wave (P_{sim}) and the DS in vacuum calculated by (2), as shown in (5)

$$P_{est} = \frac{\mathrm{DS}^2}{E_{max,sim}^2} \cdot P_{sim}. \tag{5}$$

As we know, the discontinuous abrupt structures can easily cause the enhancement of electric field, and increase the value of MFEF. The number of slots is related to the order of the high order mode, which becomes the link between the cavity mode theory and the evaluation on power capacity. Suppose the electric field of the slot is cosine distribution:

$$E\,(x, y, z) = E_a \cos kl, \tag{6}$$

and the voltage on the aperture of the slot $V_s = w_e E_a$. The minimum width of the slot (w_{min}^s) required to avoid gas breakdown can be calculated by the maximum radiation power (P_s^{max}), and is as follows:

$$w_s^{min} = \frac{V_s}{E_s} = \frac{\sqrt{P_s^{max}/G_s}}{E_s} = \sqrt{\frac{Z_0^2 P_s^{max}}{4R_d E_{max}^2}}. \tag{7}$$

where, the slot radiation conductance G_s can be determined by the duality theorem from the resonant dipole radiation resistance [29]. The maximum allowable electric field (E_s) refers to the DS in vacuum at 9.1 GHz according to formula (5). If the input power (P_{in}) is 1 GW and the return-loss is lower than -10 dB, so the slot array shall radiate power of 0.9 GW. According to the theory of cavity mode, the number of slot is equal to $a \times b$. Therefore, each slot needs to withstand the power of $0.9/ab$ GW at least, then the minimum width of the slot can be determined by

$$w_s^{min} = \sqrt{\frac{Z_0^2\,(0.9\ GW)}{4abR_d E_{max}^2}}. \tag{8}$$

It is found that the number of the slots and the simulated maximum electric field affect the power capacity of the slotted cavity antenna.

B. ANALYSIS OF CAVITY MODES

Theory of cavity mode is derived by EM wave equations. As seen in Fig. 5, when dimensions along the axis direction of rectangular cavity is certain, then all eigenmodes can be determined. It is assumed that the filled material of the cavity is air ($\epsilon_r = \mu_r = 1$), the propagation constant k and the wave number β of the rectangular cavity can be calculated by

$$\beta = \sqrt{k_c^2 - k^2} = \sqrt{\left(\frac{m\pi}{a}\right)^2 + \left(\frac{n\pi}{b}\right)^2 - k^2}, \tag{9}$$

and the corresponding cutoff frequency of the rectangular cavity is given by

$$f_{mnp} = \frac{\omega_{mnp}}{2\pi\sqrt{\mu\epsilon}} = \frac{1}{\mu\epsilon}\sqrt{\left(\frac{m\pi}{2a}\right)^2 + \left(\frac{n\pi}{2b}\right)^2 + \left(\frac{p\pi}{2l}\right)^2}, \tag{10}$$

where, m, n and p correspond to the subscript of high order mode which is defined along x, y and z-*axis*, respectively. It approximately means TE_{mn0} mode can be considered as a uniform distribution of $m \times n$ TE_{10} modes in the *xoy* plane. μ and ϵ are permeability and permittivity of air, respectively. a, b, c are length, width and height of the rectangular cavity, respectively. If $a = b$, the degenerate mode in pairs may exist simultaneously in the cavity due to the symmetric boundary conditions. High order modes in [30] have been reported, which can be combined into a new hybrid mode to improve the radiation performance. The obvious shortage in the symmetry of the far field pattern shall be paid attention [31], [32]. Since the alternately arranged slot are introduced, the symmetry of E-plane far field pattern will degenerate when m and n are both odd number. The AHOM TE_{540} [26] and hybrid mode TE_{320} [30] have been reported to improve the symmetry of the far field pattern at E-plane. Therefore, the odd order number along to the E-plane of high order mode must be selected.

Fig. 6 shows the response of high order modes to the dimension of the cavity calculated by (10). There are several other higher IMs in pairs close to the frequency of

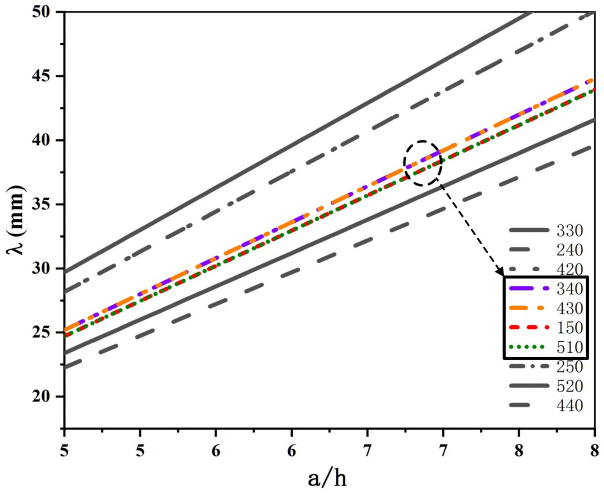

FIGURE 6. Frequency response of high order modes.

TE_{430} mode. Obviously, the distance between the degenerate mode (TE_{150} mode and TE_{510} mode) and the operating mode (TE_{430} mode) is the closest(marked by a circle in Fig. 6). Modes with similar cutoff frequencies are easy to interfere with each other. It must be ensured that IMs and TE_{430} mode are not simultaneously excited.

IV. DESIGN OF DOUBLE-LAYER SLOTTED CAVITY ANTENNA

A. ESTIMATION ON POWER CAPACITY OF SLOTS

Before the design of the antenna, it is required to estimate the power capacity of slots according to the operating mode to prevent air breakdown. As mentioned above, the number of slots and the parity of high order modes affect the power capacity of the slotted cavity antenna and the symmetry of far field pattern, respectively. It is concluded that the higher the order of the mode, the greater the power capacity. Since the aperture dimension of the antenna is determined by the operating frequency, TE_{430} mode is selected as an AHOM in making compromise between the power capacity and the aperture area of the antenna. Suppose the power of the incident EM wave from the MILO source is 1 GW, and the power distribution ratio of TE_{430} mode is 1:12, then the required power handling capability of each slot must be 83.3 MW. Bring a and b into (10), the theoretical minimum width of slot at 9.1 GHz can be obtained by

$$w_{unit} \geq 2.4\ mm. \tag{11}$$

B. CHESSBOARD METHOD

The eigenvalue can be derived from the electric field component of TE_{mnp} mode in the rectangular cavity. For a low profile, let p be zero, which can be ignored in the derivation process. Then, expressions of TE_{mn0} mode of the rectangular cavity are as follows:

$$H_z\,(x, y, z) = H_m \cos\left(\frac{m\pi}{a}x\right)\sin\left(\frac{n\pi}{b}y\right);$$

$$
\begin{aligned}
H_x(x,y,z) &= \frac{-1}{k_c^2}\left(\frac{mn\pi^2}{ab}\right)H_m \sin\left(\frac{m\pi}{a}x\right)\cos\left(\frac{n\pi}{b}y\right);\\
H_y(x,y,z) &= 0;\\
E_z(x,y,z) &= \frac{-j\omega\mu}{k_c^2}\left(\frac{m\pi}{a}\right)H_m \sin\left(\frac{m\pi}{a}x\right)\sin\left(\frac{n\pi}{b}y\right);\\
E_x(x,y,z) &= E_y(x,y,z) = 0.
\end{aligned} \tag{12}
$$

Since the electric field only have z-axis component, analysis of the high order mode can be simplified as the following chessboard method. Based on the completeness of eigenmodes, the total normalized electric field distribution ($\tilde{E}_{total}$) can be expressed as

$$
\begin{aligned}
\tilde{E}_{total} &= \sum_{i=1}^{N} a_i \tilde{E}_i \\
&= a_1\tilde{E}_1 + a_2\tilde{E}_2 + \cdots + a_N\tilde{E}_N \\
&= \sum_{\substack{i=1 \\ (m,n)=(1,0)}}^{N,(N,N)} a_i(-\frac{j\omega\mu}{k_c^2})(\frac{m\pi}{a})\sin(\frac{m\pi}{a}x)\sin(\frac{n\pi}{b}y)
\end{aligned} \tag{13}
$$

where, $\tilde{E}_i$ is the normalized electric field component of arbitrary eigenmode. Assuming that each mode is excited by equal magnitude, then the normalized coefficient $a_i = 1$. The sequence of eigenmode is arranged according to the cutoff frequency, determined by m and n.

Based on the orthogonality of eigenmodes, each independent orthogonal mode expresses as a set of N order vector (for instance, $(1, 0, \cdots, 0)$ is for TE_{10} mode, and degenerate modes have the same vector), which means each solution of the total electric field corresponds to a set of normalized independant coefficient vector. Therefore, $\tilde{E}_{\text{total}}$ can be expressed as the combination of a series of vectors. Note that elements of the vector can only be 0 or 1, due to normalization.

As discussed above, each eigenmode can be represented as a set of vector, as well as a unique field plot. To simplify the analysis, the field plot is meshed, positions of peaks and troughs are replace by '+' and '−', respectively. As seen in Fig. 7, the field plot is converted into the chessboard plot. If two modes overlap, the corresponding chessboard plots follow the principle of 'in-phase retention, and reverse cancellation', as seen in Fig. 7 (a)-(b). Therefore, the chessboard plot helps to achieve a fast design process. Especially, when the high order mode is determined, the location of the feedline can be determined quickly.

Since the radius of the terminal face is far more than $\lambda_g/2$, which is unable to match the electric field of TE_{430} mode with the transverse electric field distribution of the overmoded CWG. Therefore, the means of probe feed method is no longer applicable. The electric field distribution of the overmoded CWG without slots is shown in Fig. 8 (a), the slotted version are shown in Fig. 8 (b). The red dot marks show the location of the feed structure, and the polarization of electric

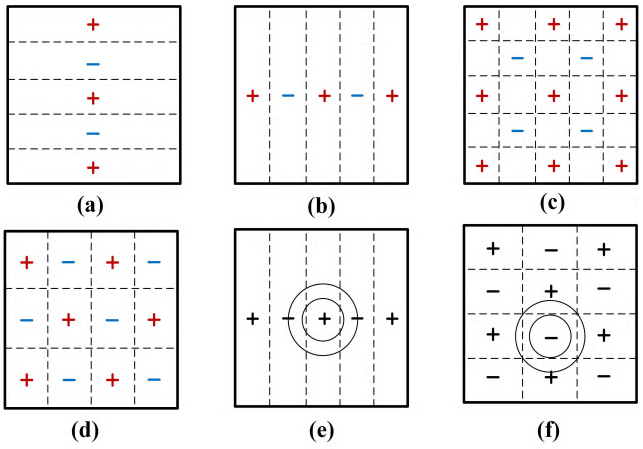

FIGURE 7. Chessboard plots of high order modes: (a) TE_{150} mode; (b) TE_{510} mode; (c) hybrid mode of TE_{150} and TE_{150}; (d) operating mode TE_{430}; (e) TE_{510} mode and position of the overmoded CWG; (f) TE_{430} and position of the overmoded CWG.

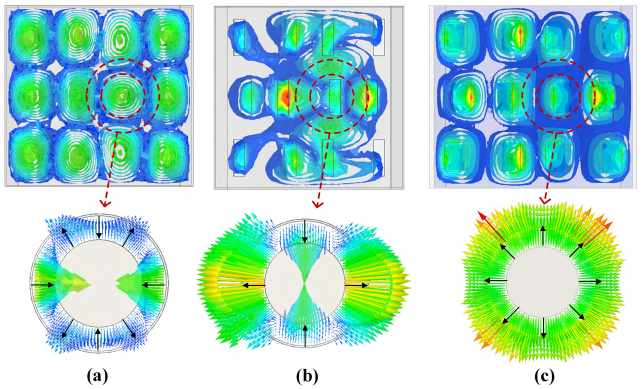

FIGURE 8. E-Field distribution of the cavity and the overmoded CWG: (a) single unslotted cavity; (b) single layer slotted cavity; (b) double-layer slotted cavity.

field is indicated by the black arrow. The figure shows that TE_{41} and TE_{21} mode exist in the overmoded CWG when the unslotted and slotted cavity is introduced, respectively. It is concluded that IMs (degenerate mode of TE_{150} and TE_{510} mode) in the slotted cavity can be excited by TE_{21} mode when the overmoded CWG is used as a feedline. In the next chapter, an innovative double-layer cavity is used to suppress TE_{21} mode.

C. DESIGN OF DOUBLE-LAYER CAVITY WITH DUAL MODE

The overmoded CWG is chosen to improve the power capacity of the transmission waveguide, which ensures the HPM energy propagates without air breakdown. In this paper, dimensions of the inner and outer conductor are 11.8 mm and 17 mm, respectively. The overmode ratio of the overmoded CWG is lower than that of the standard CWG, which means the oversized feedline will be mismatch easily as it cascades with other devices. The detailed reason has been discussed in the previous chapter.

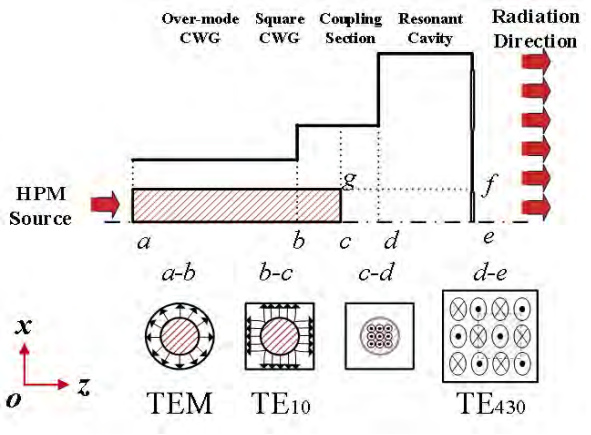

FIGURE 9. Cross-Section view of the conformal slotted cavity.

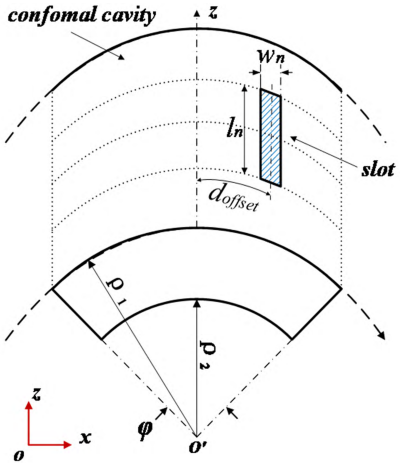

FIGURE 10. sketch of the conformal slotted cavity.

A double-layer slotted cavity (the upper is slotted cavity, the lower is rectangular cavity) is introduced to suppress TE_{21} mode, the longitudinal-section and cross-section diagram are shown in Fig. 9. The whole structure consists of the overmoded CWG (a-b), the rectangular cavity (b-d) and the slotted cavity (d-e). As seen in Fig. 8 (c), it is obviously that the transmission mode of RWG is no longer TE_{21} mode, which is suppressed by the strong linear polarization of RWG working in TE_{10} mode. TE_{21} mode in the overmoded CWG has been turned into TEM mode by the rectangular cavity. Moreover, the electric field distribution excited by TE_{10} mode has a better uniformly magnitude than one excited by TE_{41} and TE_{21} mode, as seen in Fig. 8 (a) and (b), respectively.

D. SHAPED BEAM BASED ON CONFORMAL SLOT ARRAY THEORY

As an HPM feed antenna, circular aperture is not suitable for the shaped reflectarray. Because the highest aperture efficiency can be obtained only when the power one in the center [33]. However, the currently paper reported HPM feed antenna only obtains the circular or elliptical beam, which can hardly achieve the highest aperture efficiency while illustrating the shaped reflector.

Due to the curve profile, the conformal array is different from the planar array [34]. Suppose the reflectarray is fed in-phase and uniform excitation, the plane EM wave has a extra spatial phase difference owing to the different distance from each unit to the according projection aperture of the feed antenna. The spatial phase difference is related to the vertical distance from the array aperture to the projection surface d_n and the propagation constant k ($k = 2\pi/\lambda$). In Fig. 10, the curvature angle is φ, diameters of the upper and lower cavity are expressed as ρ_1 and ρ_2, respectively. The length, width and offset of slot are l_n, w_n and d_{offset}, respectively.

For the linear array, suppose radiation units are identical and have the same spacing distance, all units point to the same direction. Then, the far field pattern in the azimuth plane is the product of the unit factor and the array factor. Let spacing distance be d, and assumes that the array is uniform excitation. The phase shift of the subsequent unit is related to the prior beam direction, then the radiation function of the linear array is shown as below

$$E(\theta) = EL(\theta) \sum_n E_n e^{jnd \sin\theta}, \tag{14}$$

where, E_n is the excitation of the nth unit, θ is the angle between the vertical direction of the linear array and a certain position of the far field. The element factor $EL(\theta)$ is common to all elements and can be therefore brought outside the summation sign in this equation. The radiation function is the product of the element factor and the array factor. The unit factor is uniform to all units and is therefore brought outside the summation sign in above equations. The latter unit has a lag phase $\psi_n = kndsin\theta$ with respect to the prior one, the first unit is seen as the zero phase point with respect to all latter units, which means that the beam direction of the first unit is the reference phase plane.

Following the above principle, the shift phase ψ_n of the nth unit can be confirmed by determining the reference phase plane of the circle array which simplifies the calculation process. Similarly, it is assumed that the reference phase plane goes through the center of the circle, and is vertical to the central axis of the circle array (as seen in Fig. 11). After the simple geometric operations, the radiation function of the conformal array can be shown as

$$E(\theta) = \sum_n E_n EL(\theta - n\Delta\varphi) e^{jkR\cos(\theta - n\Delta\varphi)}, \tag{15}$$

where, $\Delta\varphi$ is the segmental angle of $\varphi/(N-1)$ radian. The radius R can be calculated by the arc length and the curvature. The phase has been referenced to the center of the circle. The identical elements are spaced $R\Delta\varphi$ along the circle, each element points in the radial direction, as seen in Fig. 11. The element function can, therefore, in general not be brought outside the summation sign, since it is a function of the element position, there is no common element factor.

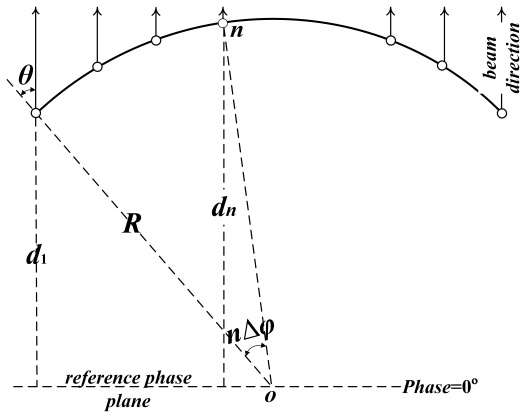

FIGURE 11. Schematic of conformal array.

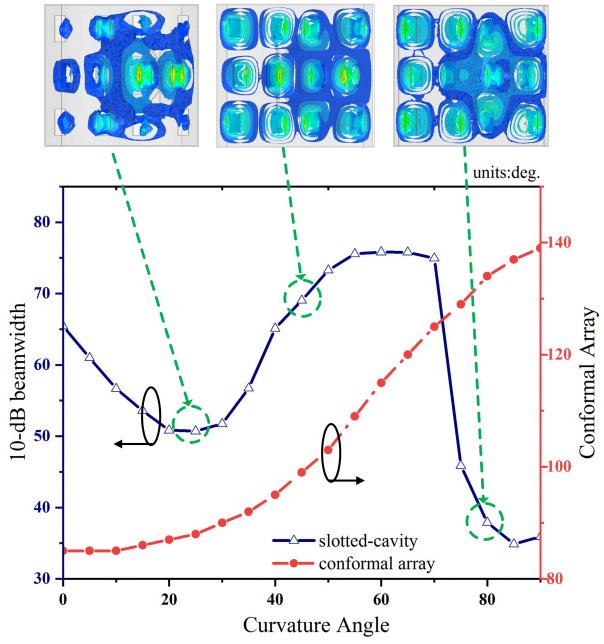

FIGURE 12. Response of the beamwidth to curvature angle.

No articles has reported the conformal array theory applied in feed antenna in HPM to improve the 10-dB beamwidth and achieve the shaped beam. Due to the discontinuity of the overmoded CWG, it is hard to excite a pure high order mode (TE_{430}) in the single slotted cavity antenna, a conformal slotted cavity working in dual mode is introduced, resulting in suppressing TE_{21} mode or other IMs and realizing the effective axial radiation. A ideal circular slot array and the slotted cavity antenna are simulated by business mathematics software (MatLab) and commercial microwave simulation software (HFSS), respectively. The response of the 10-dB beamwidth with different curvature is obtained, as seen in Fig. 12.

The simulation results show that the 10-dB beamwidth deteriorated sharp when the curvature ranges from 0° to 40° and from 70° to above. The electric field distribution of two curvature angles of 25° and 80° are shown in Fig. 12, there are high order modes excited by the overmoded CWG, almost all energy concentrated nearby the feedline. Only when the culture angle ranges from 40° to 70°, 10-dB beamwidth is consistent with the trend of the ideal conformal array, which is used as a reference range for designing the curvature of the conformal slotted cavity to achieve the shaped beam.

E. HORN-CAVITY DESIGN

For a better power handling capability, chamfer, fillet and other methods seem not sufficient to improve the power capacity of slot. The shaped slot [38] is only to make the electric field uniform in a two-dimensional plane rather than three-dimensional space. It is known that, the region exterior to the slot is treated as a parallel plate waveguide which can radiate into half space through the aperture in an infinite ground plane. In this paper, the horn-cavity makes the magnitude of electric field uniform in three-dimensional space, which significantly increases the power capacity.

The electric wall along the edge around the slot makes the aperture field more uniform, reduces the concentration of electric field, widens the aperture field of slots and relieves the mutual coupling of units [35], [36]. As seen in Fig. 13, it is found that the magnitude of electric field of slot with horn-cavity decreased. With the horn-cavity, the radiation field of slot forms a homogeneous wave front at the horn aperture, and energy is uniformly distributed.

In Fig. 13 (a), electric field of the slotted cavity antenna without horn-cavity mainly concentrates in the vicinity of slot and discontinuous abrupt structure. The simulation results show that the maximum magnitude of electric field in vacuum is 3254 V/m, the power capacity at 9.1 GHz is just 580 MW. In Fig. 13 (b), the maximum magnitude of electric field in vacuum is 2175 V/m (33% reduced), the power capacity at 9.1 GHz is above 1.29 GW.

V. PERFORMANCE OF DOUBLE-LAYER CAVITY ANTENNA

A. SIMULATION AND MEASURED RESULTS

All designs and optimized works have been done by HFSS based on the finite elements method (FEM). The far field patterns of E-plane and H-plane of the proposed antenna are shown in Fig. 16 (a) and (b) respectively. The slotted cavity is fed from the bottom surface by the single bias overmoded CWG. All dimensions are listed in Table 2. The radiation patterns are both symmetric, and the difference of the main beam between two planes is observed, the 10-dB beamwidth of E-plane and H-plane are 56.6° and 36.6°, respectively, the angle difference is less than 1°. The maximum gain difference on both sides of the main beam doesn't exceed 1 dB within the 10-dB beamwidth. The real gain (considering the return loss) of 17.03 dBi, and low side-lobes level of −14 dB is obtained. In Fig. 15, the return loss at 9.1 GHz is −37.5 dB, and the −10-dB bandwidth is 60 MHz. Within

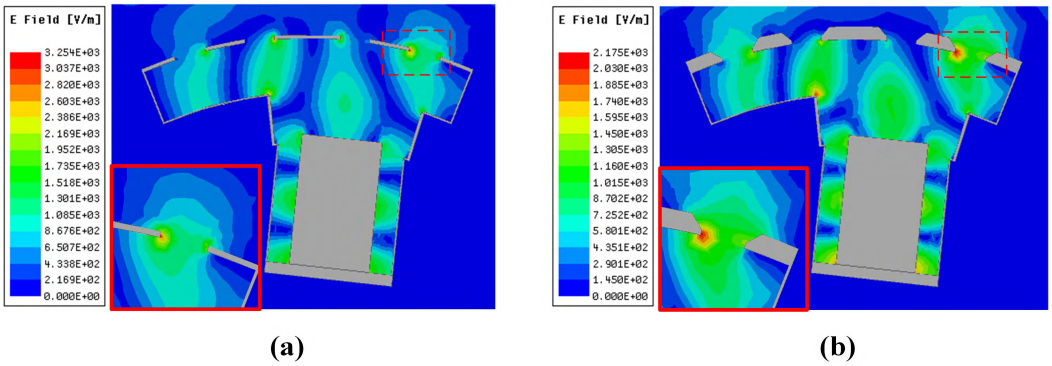

FIGURE 13. E-Field inside the antenna with or without the horn-cavity. (a) The slotted cavity antenna without horn-cavity. (b) The slotted cavity antenna with horn-cavity.

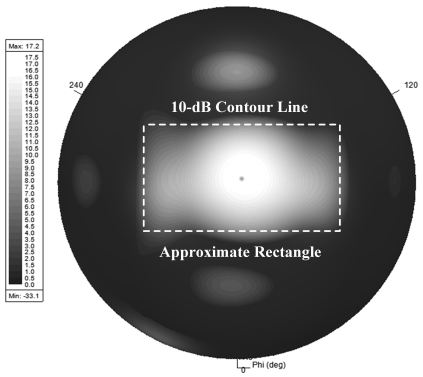

FIGURE 14. 10-dB gain contour map of the spherical section.

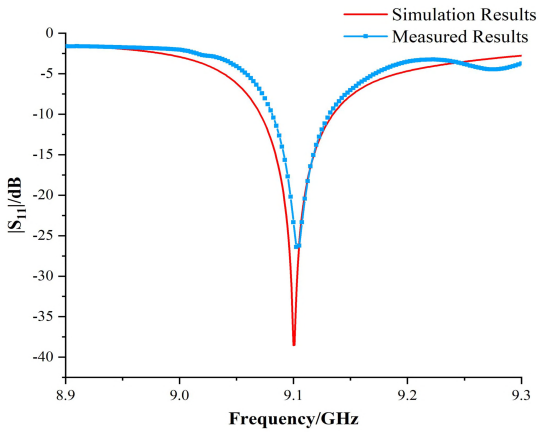

FIGURE 15. Simulation and measured reflection coefficient of the proposed HPM feed antenna.

the bandwidth, the peak radiation efficiency of 98.9% (the corresponding aperture efficiency is about 68%) is achieved.

The simulation results of the 10-dB gain contour map is shown in Fig. 14, which is a spherical section of the real gain of 10-dB. The closed contour line means the same value of real gain, when highlights the contour line of 10-dB gain, it is observed that almost all values which are equal or above 10-dB concentrate in a circle area (rectangular dotted line). As a feed antenna of the shaped reflectarray, it achieves rectangular illumination area for the highest aperture efficiency.

The experiment of the proposed antenna was completed in the far field anechoic chamber. The measured results of the reflection coefficient and far field patterns are shown in Fig. 15 and Fig. 16. It is seen in Fig. 15, the measured and simulated reflection coefficient with −10-dB bandwidth are from 9.08 GHz to 9.13 GHz, and from 9.07 GHz to 9.13 GHz, respectively. The comparison between simulated and measured far field patterns at 9.08 GHz, 9.1 GHz and 9.13 GHz are shown in Fig. 16. The measured (simulated) 10-dB beamwidth of H-plane at the three frequency are −21.6°/+18° (−18.6°/+18.6°), −17.9°/+20.2° (−18.3°/+17.9°), −19.3°/+16.4° (−17.8°/+17.8°), respectively. And, the 10-dB beamwidth of E-plane is −24.4°/+23° (−27.4°/+23.1°), −28.2°/+27.8°, (−31.6°/+31.2°), −24.9°/+26.1° (−28.1°/+22.6°), respectively. The maximum difference is lower than 3.5°. The discrepancy between simulation and measured results may be caused by the manufacture inaccuracy, assembly and install.

TABLE 2. Comparison with the common feed antenna in HPM.

Reference	Frequency	Length	Aperture	Power Capacity	Operation Modes.
Ref. 4	1.76 GHz	3.53λ	$6\lambda^2$	2.4 GW	TE_{11}
Ref. 11	4.5 GHz	4.35λ	$15.1\lambda^2$	100 MW	TE_{11}
Ref. 12	9.4 GHz	6.9λ	$51.8\lambda^2$	4 GW	HE_{11}
Ref. 13	18.85 GHz	8.18λ	$60.1\lambda^2$	526 MW	/
This work	9.1 GHz	0.82λ	$2.8\lambda^2$	1.29 GW	TEM

B. THE COMPARISON BETWEEN THE PREVIOUS AND PROPOSED WORK

The comparison between the common HPM feed antenna and the proposed feed antenna is shown in Table 2. In [4], [11]–[13]. The first four horn antenna can only operate in TE_{11} mode with mode converter, which increases the volume of the antenna. It is concluded that the proposed HPM

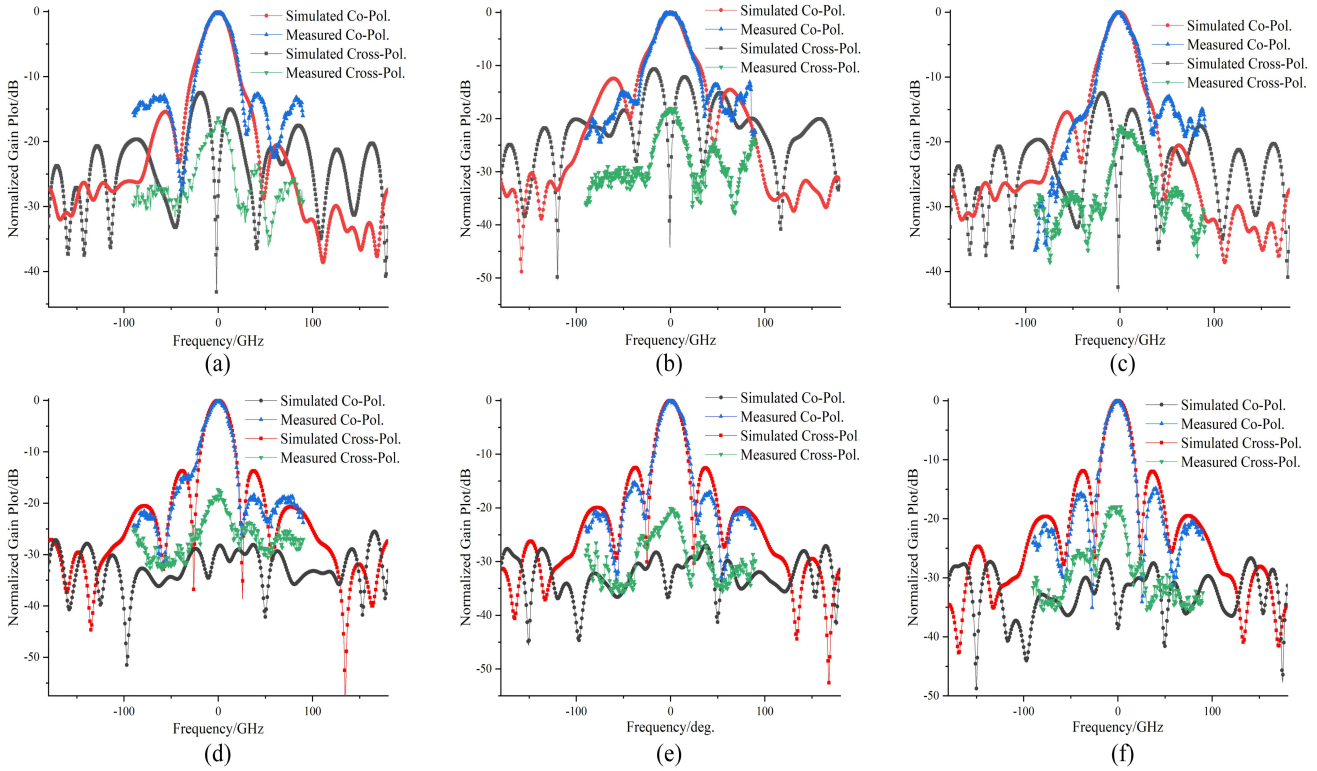

FIGURE 16. Co-polarization (Co-pol.) and Cross-polarization (Cross-pol.) pattern of the proposed antenna at E-plane and H-plane: (a) E-plane at 9.08 GHz; (b) E-plane at 9.1 GHz; (c) E-plane at 9.13 GHz; (d) H-plane at 9.08 GHz; (e) H-plane at 9.1 GHz; (f) H-plane at 9.13 GHz.

feed antenna has a more compact structure than those of traditional applications.

VI. CONCLUSION

In this paper, a conformal double-layer slotted cavity antenna as feed of the shaped reflectarray in HPM is designed and manufactured. The AHOM TE_{430} is introduced to obtain a better equalization performance of the far field pattern at E-plane, and a compact size is obtained by the slotted cavity without extra power dividers, phase shifters, and mode converters. The conformal slotted cavity working in dual mode suppresses high order mode TE_{21} caused by the overmoded CWG to excite purer high order mode TE_{430}. The shaped beam is achieved by using the conformal slotted cavity, which is suitable for the shaped reflectarray. Horn-cavity above the slot makes the electric field uniform, and improves the power handling capability. The measured results of the return loss and radiation patterns are in good agreement with the simulation results, which proves the proposed compact conformal slotted cavity antenna is a good candidate for the feed antenna in HPM.

ACKNOWLEDGMENT

Xiao Ma would like to give his appreciations to Ms. Chen for checking the article and supporting him in his life.

REFERENCES

[1] S. N. Vlasov and I. M. Orlova, "Quasioptical transformer which transforms the waves in a waveguide having a circular cross section into a highly directional wave beam," *Radiophys. Quantum Electron.*, vol. 17, no. 1, pp. 115–119, Jan. 1974.

[2] C. C. Courtney, D. E. Voss, C. E. Baum, W. Prather, and R. Torres, "A description and the measured performance of three coaxial beam-rotating antenna prototypes," *IEEE Antennas Propag. Mag.*, vol. 44, no. 3, pp. 30–47, Jun. 2002.

[3] T. Bondo and S. B. Sorensen, "Physical optics analysis of beam waveguides using auxiliary planes," *IEEE Trans. Antenn. Propag.*, vol. 53, no. 3, pp. 1062–1068, Mar. 2005.

[4] C.-W. Yuan, Y.-W. Fan, H.-H. Zhong, Q.-X. Liu, and B.-L. Qian,, "A novel mode-transducing antenna for high-power microwave application," *IEEE Trans. Antennas Propag.*, vol. 54, no. 10, pp. 3022–3025, Oct. 2006.

[5] X.-Q. Li, Q.-X. Liu, X.-J. Wu, L. Zhao, J.-Q. Zhang, and Z.-Q. Zhang, "A GW level high-power radial line helical array antenna," *IEEE Trans. Antennas Propag.*, vol. 56, no. 9, pp. 2943–2948, Sep. 2008.

[6] S. F. Wang and Y. Z. Xie, "Design and optimization of high-power UWB combined antenna based on klopfenstein impedance taper," *IEEE Trans. Antennas Propag.*, vol. 65, no. 12, pp. 6960– 6967, Dec. 2017.

[7] Y. Liang, J. Zhang, Q. Liu, and X. Li, "High-power radial-line helical subarray for high-frequency applications," *IEEE Trans. Antennas Propag.*, vol. 66, no. 8, pp. 4034–4041, Aug. 2018.

[8] C.-W. Yuan, S.-R. Peng, T. Shu, Z.-Q. Li, and H. Wang, "Designs and experiments of a novel radial line slot antenna for high-power microwave application," *IEEE Trans. Antennas Propag.*, vol. 61, no. 10, pp. 4940–4946, Oct. 2013.

[9] A. Jouade, M. Himdi, A. Chauloux, and F. Colombel, "Mechanically pattern-reconfigurable bended horn antenna for high-power applications," *IEEE Antennas Wireless Propag. Lett.*, vol. 16, pp. 457–460, 2017.

[10] A. M. Khan, M. M. Ahmed, M. Rafiq, and U. Rafique, "Design of an Efficient High Power Microwave antenna," in *Proc. 19th Int. Multi-Topic Conf. (INMIC)*, Dec. 2016, pp. 1–6.

[11] E. C. Becker, S. D. Kovaleski, and J. M. Gahl, "Optimization of a compact conical horn antenna system for high power microwaves in the 4 to 6 GHz range," *IEEE Trans. Dielectr. Elect. Insul.*, vol. 18, no. 4, pp. 1066–1070, Aug. 2011.
[12] G. Xu *et al.*, "An X-band high power microwave launcher with polarization reconfigurable capacity," *High Power Laser Part. Beams*, vol. 27, no. 10, pp. 100–104, 2015.
[13] J. Yuan, G. Hua, and K. Gao, "A high power microwave multi-modes horn antenna," *Electron. Sci. Tech.*, vol. 26, no. 7, pp. 91–93, 2013.
[14] J. H. Yang *et al.*, "Effect of air and SF_6 breakdown on transmission of high power microwave," *High Power Laser Part. Beams*, vol. 24, no. 1, pp. 1223–1227, 2005.
[15] L. Niemeyer, L. Pietronero, and H. J. Wiesmann, "Fractal dimension of dielectric breakdown," *Phys. Rev. Lett.*, vol. 52, no. 12, pp. 1033–1036, Mar. 1984.
[16] G. Deng, "High power ferrite phase shifter based on structure of waveguide in parallel," *High Power Laser Part. Beams*, vol. 28, no. 8, 2016.
[17] X. Zhao, C. Yuan, L. Liu, S. Peng, Z. Bai, and D. Cai, "GW TEM-mode phase shifter for high-power microwave applications," *IEEE Trans. Plasma Sci.*, vol. 44, no. 3, pp. 268–272, Mar. 2016.
[18] C. Chang, L. Guo, S. G. Tantawi, Y. Liu, J. Li, C. Chen, and W. Huang, "A new compact high-power microwave phase shifter," *IEEE Trans. Microw. Theory Techn.*, vol. 63, no. 6, pp. 1875–1882, Jun. 2015.
[19] Y.-W. Fan, X.-Y. Wang, H.-H. Zhong, and J.-De Zhang, "A dielectric-filled magnetically insulated transmission line oscillator," *Appl. Phys. Lett.*, vol. 106, no. 9, Feb. 2015, Art. no. 093501.
[20] S. Yang and H. Li, "Optimization of novel high-power millimeter-wave TM_{01}-TE_{11} mode converters," *IEEE Trans. Microw. Theory Techn.*, vol. 45, no. 4, pp. 552–554, Apr. 1997.
[21] S. Peng, C. Yuan, H. Zhong, and Y. Fan, "Design and experiment of a cross-shaped mode converter for high-power microwave applications," *Rev. Sci. Instrum.*, vol. 84, no. 12, Dec. 2013, Art. no. 124703.
[22] X. Cui, "High-efficiency, broadband converter from a rectangular waveguide TE_{10} mode to a circular waveguide TM_{01} mode for overmoded device measurement," *IEEE Access*, vol. 6, pp. 14996–15003, 2018.
[23] W. Lawson, "Theoretical mode conversion in overmoded nonlinear coaxial waveguide tapers," *IEEE Trans. Microw. Theory Techn.*, vol. 42, no. 1, pp. 127–131, Jan. 1994.
[24] J. Fouany, "New concept of telemetry X-band circularly polarized antenna payload for cubesat," *IEEE Antennas Wireless Propag. Lett.*, vol. 6, pp. 2987–2991, 2017.
[25] W. Han, F. Yang, J. Ouyang, and P. Yang, "Low-cost wideband and high-gain slotted cavity antenna using high-order modes for millimeter-wave application," *IEEE Trans. Antennas Propag.*, vol. 63, no. 11, pp. 4624–4631, Nov. 2015.
[26] X. Ma, F. Yang, R. Wong, M. Gao, and X. Cui, "A compact slotted-cavity antenna for HPM reflector feed," in *Proc. IEEE Int. Symp. Antennas Propag. USNC/URSI Nat. Radio Sci. Meeting*, Boston, MA, USA, Jul. 2018, pp. 1985–1986.
[27] J. A. Bossard, C. P. Scarborough, Q. Wu, S. D. Campbell, D. H. Werner, P. L. Werner, S. Griffiths, and M. Ketner, "Mitigating field enhancement in metasurfaces and metamaterials for high-power microwave applications," *IEEE Trans. Antennas Propag.*, vol. 64, no. 12, pp. 5309–5319, Dec. 2016.
[28] R. A. Jameson, "High brightness H-accelerators," in *Proc. IEEE Part. Accel. Conf.*, 1987.
[29] D. Yaoyong and Y. Chen, "Air breakdown of high power microwave pulse and its effect on transmitted energy," *J. Microw.*, vol. 16, no. 3, pp. 260–264, 2000.
[30] W. Li, K. D. Xu, X. Tang, Y. Yang, Y. Liu, and Q. H. Liu, "Substrate integrated waveguide cavity-backed slot array antenna using high-order radiation modes for dual-band applications in *K*-ban," *IEEE Trans. Antennas Propag.*, vol. 65, no. 9, pp. 4556–4565, Sep. 2017.
[31] G. Q. Luo, X. H. Zhang, L. X. Dong, W. J. Li, and L. L. Sun, "A gain enhanced cavity backed slot antenna using high order cavity resonance," *J. Electromagn. Waves Appl.*, vol. 25, nos. 8–9, pp. 1273–1279, Jan. 2011.
[32] W. Han, F. Yang, and H. Zhou, "Slotted substrate integrated cavity antenna using TE_{330} mode with low profile and high gain," *Electron. Lett.*, vol. 50, no. 7, pp. 488–490, Mar. 2014.
[33] S. Rao, L. Shafai, and S. Sharma, *Handbook of Reflector Antennas and Feed Systems*. Norwood, MA, USA: Artech House, 2013.
[34] D. G. Dudley, *Conformal Array Antenna Theory and Design*. Piscataway, NJ, USA: IEEE Press, 2006.
[35] M. Dich and S. R. Rengarajan, "Mutual coupling between waveguide-fed transverse broad wall slots radiating between baffles," *Electromagnetics*, vol. 17, no. 5, pp. 421–435, Dec. 1997.
[36] T. Suzuki, J. Hirokawa, and M. Ando, "Iteration-free design of waveguide slot array with cavities," *IEEE Trans. Antennas Propag.*, vol. 58, no. 12, pp. 3891–3897, Dec. 2010.
[37] B. D. Braaten, M. A. Aziz, S. Roy, S. Nariyal, N. F. Chamberlain, and D. E. Anagnostou, "Half-power beamwidth of a self-adapting conformal 1×4 microstrip array," in *Proc. IEEE Int. Symp. Antennas Propag.*, Jul. 2012, pp. 1–2.
[38] N. R. Devarapalli, C. E. Baum, C. G. Christodoulou, and E. Schamiloglu, "A fan-beam radiator using waveguide's narrow wall for horizontal polarization and high power," *IEEE Trans. Electromagn. Compat.*, vol. 53, no. 2, pp. 380–389, May 2011.

XIAO MA was born in Sichuan, China. He received the B.S. degree in electronic information science and technology from Shandong University, China, in 2013. He is currently pursuing the Ph.D. degree in electromagnetic field and microwave technique with the University of Electronic Science and Technology of China, Chengdu, China.

He majors in electromagnetic field and microwave technology. His research interest includes high-power microwave reflect array antenna.

FENG YANG was born in Shaanxi, China. He received the M.S. and Ph.D. degrees in electromagnetic field and microwave technology from the University of Electronic Science and Technology of China (UESTC), Chengdu, China, in 1995 and 1998, respectively, where he is currently a Professor with the Department of Electronic Engineering.

He has published more than 100 journal papers. His research interests include antenna theory and techniques, electromagnetic scattering and inverse scattering, and UWB communication.

PENG YANG was born in Yunnan, China. He received the B.S., M.S., and Ph.D. degrees in electronic engineering from the University of Electronic Science and Technology of China (UESTC), Chengdu, China, in 2001, 2008, and 2011, respectively.

From January 2009 to November 2010, he was a Research Assistant with the Department of Electrical and Electronic Engineering, The University of Hong Kong. He is currently an Associate Professor with UESTC. His research interests include antenna theory and design, and array signal processing.

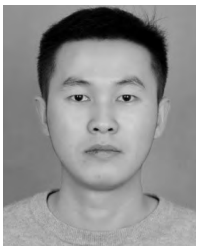

RUI WANG was born in Huaibei, Anhui, China, in 1993. He received the B.Eng. degree from the Anhui University of China, Hefei, China, in 2015. He is currently pursuing the Ph.D. degree in electromagnetic and microwave technology with the University of Electronic Science and Technology of China, Chengdu, China.

His current research interests include multibeam feed network and metasurface reflector antennas.

YI YAN was born in Anhui, China, in 1991. He received the B.S. degree in electromagnetic field and microwave technique from the University of Electronic Science and Technology of China, Chengdu, China, in 2014, where he is currently pursuing the Ph.D. degree.

His current research interests include the theory of characteristic mode and terminal antenna.

KEXIU CHEN was born in Sichuan, China, in 1992. She received the B.S. degree in communication and information technology from Dalian Maritime University, Dalian, China, in 2014, and the M.S. degree from the National Key Laboratory of Science and Technology on Communication, University of Electronic Science and Technology of China, Chengdu, China, in 2017.

Her current research interests include D2D communication applied in 5G and analysis of satellite communications.